



Contents lists available at ScienceDirect

## International Journal of Pharmaceutics

journal homepage: [www.elsevier.com/locate/ijpharm](http://www.elsevier.com/locate/ijpharm)

## Estimation of effective intestinal membrane permeability considering bile micelle solubilisation

Kiyohiko Sugano\*

Global Research &amp; Development, Sandwich Laboratories, Research Formulation, Pfizer Inc., CT13 9NJ, Sandwich, Kent, UK

## ARTICLE INFO

## Article history:

Received 8 August 2008  
 Received in revised form 1 October 2008  
 Accepted 3 October 2008  
 Available online 15 October 2008

## Keywords:

Oral absorption  
 Low solubility  
 Bile micelles  
 Unstirred water layer  
 Simulation

## ABSTRACT

In this study, the calculation method of effective intestinal membrane permeability ( $P_{\text{eff}}$ ) for bile micelle solubilised drugs was investigated. The intestinal membrane permeation is the tandem process of unstirred water layer (UWL, superimposes to the mucus layer) and epithelial cell membrane permeation. In most cases of lipophilic compounds, UWL permeation is the rate-limiting step. Four scenarios of UWL permeation were investigated: (A) only free drug permeates the UWL by self-diffusion, (B) both free drug and micelle bound drug permeate through the UWL by self-diffusion, (C) water convection carries the drug in addition to (B), and (D) both free drug and bile micelle bound drug permeate through the UWL by self-diffusion with the diffusion coefficient of the free monomer. Using danazol as a model drug, the simulation results of the four scenarios were compared with the observed fraction of a dose absorbed (Fa%) in fasted and fed state humans (fasted: 11–25%, fed: 44–72%). Scenario (A) largely underestimated the fraction of a dose absorbed (2% and 2% for fasted and fed, respectively). Scenarios (B) and (C) predicted the Fa% appropriately (B: 8% and 43%, C: 17% and 60%). Scenario (D) overestimated the Fa% (62% and 99%). The relationship between octanol–water partition coefficient and  $P_{\text{eff}}$  was also investigated.

© 2008 Elsevier B.V. All rights reserved.

### 1. Introduction

Computational oral absorption simulation is expected to be an effective tool in drug discovery and development (Jones et al., 2006; Kuentz et al., 2006; Parrott and Lave, 2002; Takano et al., 2006; Sugano et al., 2007). In the current drug discovery paradigm, the number of low solubility compounds is increasing (Lipinski, 2000; Sugano et al., 2007). Therefore, oral absorption simulation for low solubility compound is currently extensively investigated. In the case of low solubility compounds, bile micelle solubilisation in the small intestine plays an important role for oral absorption.

However, there are discrepancies between the theories and the experimental observations for bile micelle solubilised drugs: (1) in several reports of oral absorption simulation for low solubility drugs, the total concentration in bile micelle media (free drug + micelle bound drug) and membrane permeability of free monomer (e.g., obtained from Caco-2 cell assay) were simultaneously used for simulation, resulting in appropriate *in vivo* prediction (corresponding to scenario D described below) (Jones et al., 2006; Takano et al., 2006). However, in theory, when the permeability value of free monomer is used, the concentration of free

molecule (free fraction) should be used instead of the solubility in bile micelle media. (2) It is well known that many low solubility compounds undergo the positive food effect, due to the increase of solubility by bile micelles (Gu et al., 2007). However, if only free monomer molecules are available for permeation, there should be no positive food effect, since solubilisation by bile micelles does not increase the free monomer concentration. Therefore, it is of great interest to investigate the reason for these discrepancies.

The intestinal membrane permeation is the tandem process of unstirred water layer (UWL) and epithelial cellular membrane permeation (Fig. 1). The unstirred water layer superimposes to the mucus layer. In most cases of lipophilic compounds (the octanol–water distribution coefficient ( $\log D_{\text{oct}} > 2-3$ ), cellular membrane permeation is very rapid. Therefore, UWL permeation would be the rate-limiting step for lipophilic compounds (Avdeef et al., 2007; Fagerholm and Lennernaes, 1995; Lennernaes, 2007a; Obata et al., 2005; Sugano et al., 2003; Youdim et al., 2003).

Previously, it was suggested that bile micelles can permeate through the UWL by self-diffusion, and therefore, bile micelles work as the carrier of a compound (Amidon et al., 1982; Li et al., 1996). Micelles from self-emulsifying drug delivery system (SEDDS) formulation were also suggested to permeate through the UWL (Araya et al., 2006; Porter et al., 2007). In addition, it is well known that nano-scale particles (ca <500 nm) can permeate through the mucus layer (Norris and Sinko, 1997; Sanders et al., 2000). The effect of

\* Tel.: +44 1304 644338.

E-mail address: [Kiyohiko.Sugano@pfizer.com](mailto:Kiyohiko.Sugano@pfizer.com).

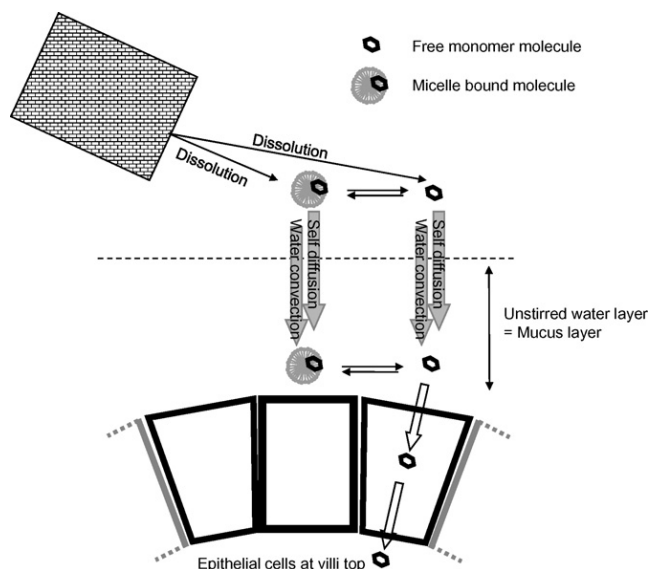


**Fig. 1.** Schematic presentation of intestinal membrane permeation. Both free monomer molecule and micelle bound molecule can permeate the unstirred water layer. The equilibrium between the monomer and micelle bound molecule are rapid and free monomer fraction permeate the epithelial membrane.

water convection on UWL permeability has been suggested in addition to self-diffusion (Nilsson et al., 1994; Pappenheimer, 2001). However, UWL permeation of a bile micelle bound drug has not been considered in oral absorption simulation.

In this study, four scenarios of UWL permeation were considered (Fig. 1).

- Only free monomer molecule (free fraction) permeates the UWL by self-diffusion.
- Both free monomer molecules and bile micelle bound molecules permeate across the UWL by self-diffusion.
- (B) plus convection accompanying water absorption (water convection).
- Both free drug and bile micelle bound drug permeate through the UWL by self-diffusion with the diffusion coefficient of the free monomer.

The predicted values of the fraction of a dose absorbed (Fa%) by the four scenarios were compared with the clinical oral absorption data for danazol, a typical low solubility compound.

## 2. Theory

### 2.1. $P_{eff}$ equation

In the case of a low solubility compound, solubility in the intestinal fluid is often increased by bile micelles. In this study, the effective concentration for permeation in the intestinal fluid ( $C_{eff}$ ) is defined as the sum of the concentrations of free molecules and the bile micelle bound molecules (Sugano et al., 2007). The absorption rate ( $dX_{abs}/dt$ ) can be described as

$$\frac{dX_{abs}}{dt} = SA_{si} P_{eff} C_{eff} = \frac{SA_{si}}{V_{si}} P_{eff} C_{eff} V_{si} = k_a X_{eff} \quad (1)$$

where  $SA_{si}$  is the effective surface area of the small intestine,  $P_{eff}$  is the effective intestinal membrane permeability,  $V_{si}$  is the effective volume of the intestinal fluid,  $k_a$  is the absorption rate constant ( $=SA_{si}/V_{si} \times P_{eff}$ ), and  $X_{eff}$  is the drug amount which is available for permeation ( $C_{eff} \times V_{si}$ ).

The human small intestine has a fold and villi structure. The UWL is on the top of the villi structure. Therefore,  $P_{eff}$  can be described as

$$\begin{aligned} \frac{1}{P_{eff}} &= \left( \frac{1}{P_{ep,eff}} + \frac{1}{P_{UWL,eff}} \right) \frac{1}{FE} \\ &= \left( \frac{1}{Acc VE f_{mono} P_{ep}} + \frac{1}{P_{UWL,eff}} \right) \frac{1}{FE} \end{aligned} \quad (2)$$

where  $P_{ep,eff}$  is the effective epithelial cellular membrane permeability ( $=Acc \times VE \times f_{mono} \times P_{ep}$ ),  $P_{ep}$  is the epithelial cellular membrane permeability of free monomer,  $f_{mono}$  is the fraction of free monomer,  $P_{UWL,eff}$  is the effective UWL permeability,  $Acc$  is the accessibility to the villi surface,  $VE$  is the surface expansion by villi structure ( $VE = 10$  in humans) (DeSesso and Jacobson, 2001; Oliver et al., 1998), and  $FE$  is the surface expansion by fold structure ( $FE = 3$  in humans) (DeSesso and Jacobson, 2001).  $Acc$  depends on  $P_{ep}$ ,  $f_{mono}$ , the effective diffusion coefficient in the UWL ( $D_{UWL,eff}$ ) and the permeability by water convection ( $P_{WC}$ ).  $Acc$  was calculated according to the reference (Oliver et al., 1998). In this equation, it was assumed that only free monomer molecules can permeate the epithelial membrane.

$P_{UWL,eff}$  of the above four scenarios A–D can be represented as Eqs. (3)–(6), respectively:

$$P_{UWL,eff} = \frac{f_{mono} D_{UWL,mono}}{h_{eff}} \quad (3)$$

$$P_{UWL,eff} = \frac{D_{UWL,eff}}{h_{eff}} = \frac{1}{h_{eff}} (f_{mono} D_{UWL,mono} + f_{mic} D_{UWL,mic}) \quad (4)$$

$$\begin{aligned} P_{UWL,eff} &= \frac{D_{UWL,eff}}{h_{eff}} + P_{WC,eff} = \frac{1}{h_{eff}} (f_{mono} D_{UWL,mono} + f_{mic} D_{UWL,mic}) \\ &\quad + (f_{mono} P_{WC,mono} + f_{mic} P_{WC,mic}) \end{aligned} \quad (5)$$

$$P_{UWL,eff} = \frac{D_{UWL,mono}}{h_{eff}} \quad (6)$$

where  $h_{eff}$  is the effective thickness of the UWL,  $f_{mic}$  is the fraction of micelle bound molecule ( $1 - f_{mono}$ ),  $D_{UWL,mono}$  and  $D_{UWL,mic}$  are the diffusion coefficients of free monomer and micelle bound molecules in the UWL, respectively, and  $P_{WC,mono}$  and  $P_{WC,mic}$  are the permeability of free monomer and micelle bound molecules by water convection, respectively.

#### 2.1.1. Calculation of intrinsic epithelial membrane permeability

$P_{ep}$  for undissociated molecular species was estimated from the relationship between the octanol–water partition coefficient ( $P_{oct}$ ) and the Caco-2 intrinsic membrane permeability of undissociated molecular species ( $P_{caco,int}$ ) as

$$P_{ep} = P_{caco,int} = AP_{oct}^B \quad (7)$$

where  $A$  and  $B$  are  $2.36 \times 10^{-6}$  and 1.10 respectively (Fig. 2) (Avdeef et al., 2005).  $P_{ep}$  of danazol ( $\log P_{oct} = 4.2$ ) (Glomme et al., 2006) was calculated to be 0.098 cm/s.

#### 2.1.2. Calculation of free monomer fraction

The  $f_{mono}$  can be calculated as

$$f_{mono} = \frac{S_{buffer}}{S_{micelles}} \quad (8)$$

where  $S_{micelles}$  is the solubility in biorelevant media with bile micelles and  $S_{buffer}$  is the solubility in the buffer without bile micelles. The measured solubility values in the fasted state and fed simulated intestinal fluid (FaSSIF and FeSSIF, respectively) were used for simulation (Galia et al., 1998; Vertzoni et al., 2004). FaSSIF

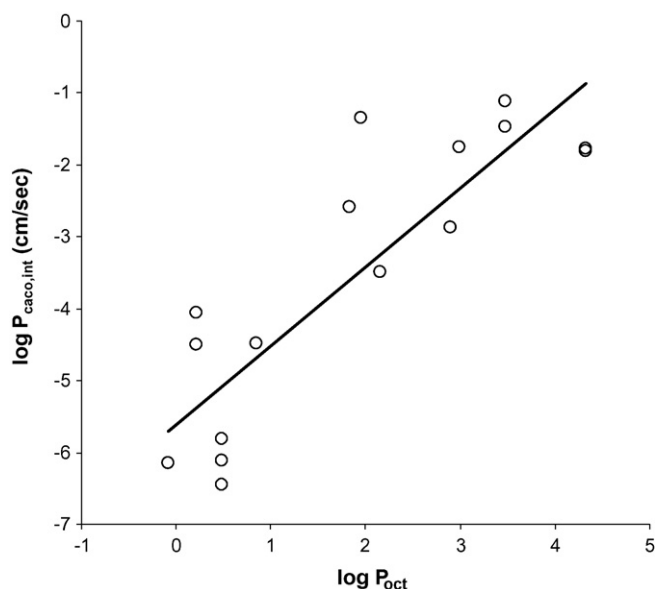


Fig. 2.  $\log P_{\text{caco,int}}$  vs Caco-2 intrinsic permeability. Data obtained from Avdeef et al. (2005).  $P_{\text{caco,int}}$  is the permeability of undissociated species in Caco-2 assay  $P_{\text{caco,int}} = 2.36 \times 10^{-6} \times P_{\text{oct}}^{1.1}$ .

and FeSSIF consist of taurocholic acid (TC) and egg lecithin (EL): TC/EL = 3 mM/0.75 mM for FaSSIF and TC/EL = 15 mM/3.75 mM for FeSSIF. The solubility values of danazol in buffer, FaSSIF and FeSSIF are 0.00021, 0.018 and 0.047 mg/mL, respectively (Okazaki et al., 2008). The  $f_{\text{mono}}$  was calculated to be 0.012 and 0.0045 in FaSSIF and FeSSIF, respectively. Previously, Glomme et al. (2006) proposed an equation to estimate  $S_{\text{micelles}}$  of TC/EL micelles from  $\log P_{\text{oct}}$  for undissociable compounds

$$S_{\text{micelles}} = S_{\text{int}} \left( 1 + \frac{C_{\text{bile}}}{C_{\text{water}}} 10^{\log K_{\text{bm}}} \right) \quad (9)$$

$$\log K_{\text{bm}} = 0.75 \log P_{\text{oct}} + 2.27 \quad (10)$$

where  $S_{\text{int}}$  is the intrinsic solubility,  $K_{\text{bm}}$  is the bile micelle–water partition coefficient,  $C_{\text{bile}}$  is the concentration of taurocholic acid, and  $C_{\text{water}}$  is the concentration of water (55.55 M).

### 2.1.3. Diffusion coefficients of free monomer and bile micelles in UWL

$D_{\text{mono}}$  of danazol was set to be  $8 \times 10^{-6} \text{ cm}^2/\text{s}$  (Okazaki et al., 2008). The diffusion coefficients of bile micelles in FaSSIF and FeSSIF were  $0.12 \times 10^{-6} \text{ cm}^2/\text{s}$  and  $1.05 \times 10^{-6} \text{ cm}^2/\text{s}$ , respectively (the bile micelle diameters were 54.4 nm and 6.3 nm, respectively) (Okazaki et al., 2008). It was reported that the mucus layer only slightly affected the diffusion coefficient of bile micelles at TC > 10–20 mM range, whereas mucus layer increases the diffusion coefficient more than 3-fold at TC < 10–20 mM range (Li et al., 1996). Therefore, for fasted state,  $0.36 \times 10^{-6} \text{ cm}^2/\text{s}$  was used, whereas the same value ( $1.05 \times 10^{-6} \text{ cm}^2/\text{s}$ ) as in the buffer was used for fed state (Li et al., 1996).

### 2.1.4. Thickness of the unstirred water layer

The apparent thickness of the UWL ( $h_{\text{app}}$ ) has been calculated from  $P_{\text{eff}}$  and  $D_{\text{UWL,eff}}$  for UWL limited permeation compounds using Eq. (2) assuming  $P_{\text{ep,eff}} \gg P_{\text{UWL,eff}}$  and FE = 1, as

$$h_{\text{app}} = \frac{D_{\text{UWL,eff}}}{P_{\text{eff}}} \quad (11)$$

Lennernas et al. reported  $h_{\text{app}}$  to be ca. 100  $\mu\text{m}$  in humans (Fagerholm and Lennernaes, 1995; Lennernaes, 2007a). However,

Eq. (11) does not consider the fold structure. If the fold structure is considered, the mucus thickness on the villi is ca. 300  $\mu\text{m}$ . This value is in good agreement with the thickness of the mucus layer obtained by direct measurements (170–480  $\mu\text{m}$  in the small intestine) (Atuma et al., 2001). In this study, 300  $\mu\text{m}$  was used as  $h_{\text{eff}}$ .

### 2.1.5. Estimation of UWL permeability by water convection

Lennernas et al. reported that the water absorption rate was  $1.3 \pm 3.0$ ,  $2.6 \pm 2.2$ , and  $3.7 \pm 3.5 \text{ mL/h/cm}$  for each experiment (Fagerholm et al., 1999; Lennernaes et al., 1994; Nilsson et al., 1994). Lambert et al. (1997) reported the water absorption was 3.3 mL/h/cm in the jejunum and much higher in the duodenum. On average, the water absorption is 2.7 mL/h/cm/GI length in humans, which corresponds to  $0.69 \times 10^{-4} \text{ cm/s}$  (based on the intestinal tube radius ( $r_{\text{GI}}$ ) of 1.75 cm, 1 cm GI length = 11.0  $\text{cm}^2$ ). This value is based on the smooth tube surface area same as  $P_{\text{eff}}$  calculation. Considering the 3-fold expansion by the fold structure,  $P_{\text{WC,eff}} = 0.23 \times 10^{-4} \text{ cm/s}$  was used for UWL permeability calculation in this study. This value was used for the permeability by water convection for both monomer and micelle bound drug ( $P_{\text{WC,eff}} = P_{\text{WC,mono}} = P_{\text{WC,mic}}$ ).

## 3. Oral absorption simulation

A compartment transit absorption model consisting of nine compartments (1 for the stomach, 7 for the small intestine, and 1 for the colon) was used for oral absorption simulation (Haruta et al., 1998; Jinno et al., 2006; Yu and Amidon, 1999). Dissolution and absorption in the stomach and colon were neglected in the same way as in previous reports (Jones et al., 2006; Kuentz et al., 2006; Parrott and Lave, 2002; Takano et al., 2006). Dissolution in the small intestine was simulated by the Nernst–Brunner equation (NBE) as previously reported (Okazaki et al., 2008). Log-normal distribution of particle size was assumed with  $d_{50} = 4.46 \mu\text{m}$  (Sunesen et al., 2005b) and standard deviation of 0.693 log unit. Spherical particle shape was assumed. The dissolution of danazol was reported to be simulated appropriately by this method (Okazaki et al., 2008).

Transfer of particles was simulated by assigning 100 virtual particles to each particle size bin. In this way, the transfer of particles and the reduction of particle radius by dissolution could be simultaneously taken into account. First-order kinetics with  $T_{1/2} = 10 \text{ min}$  and  $T_{1/2} = 30 \text{ min}$  were used for stomach emptying in fasted state and fed state, respectively (Sugito et al., 1990). The total intestinal transit time was set to be 3.5 h ( $T_{1/2} = 21 \text{ min}$  for each small intestine compartment) (Yu, 1999).

$P_{\text{eff}}$  was converted to absorption rate constant ( $k_a$ ) as

$$k_a = \frac{SA_{\text{si}}}{V_{\text{si}}} P_{\text{eff}} = \text{SVR} P_{\text{eff}} = \frac{2DF}{r_{\text{GI}}} P_{\text{eff}} \quad (12)$$

where SVR is the surface/volume ratio ( $=SA_{\text{si}}/V_{\text{si}}$ ), and DF is the degree of flatness of the intestinal tube (DF = 1 for a cylindrical tube) (Chiou, 1994). SVR can be obtained from the relationship between Fa% and  $P_{\text{eff}}$  using low permeability-high solubility drugs, assuming that colonic absorption is negligible (Fagerholm et al., 1997; Sutton et al., 2006) and the mean transit time through the small intestine ( $T_{\text{si}}$ ) is 3.5 h. Fa% can be expressed as Eq. (13) by assuming the seven-compartment model (Yu et al., 1996)

$$\begin{aligned} \text{Fa\%} &= \left( 1 - \left( 1 + \frac{k_a T_{\text{si}}}{7} \right)^{-7} \right) 100 \\ &= \left( 1 - \left( 1 + \frac{\text{SVR} P_{\text{eff}} T_{\text{si}}}{7} \right)^{-7} \right) 100 \end{aligned} \quad (13)$$

Eq. (13) was fitted to the  $F_a$ – $P_{\text{eff}}$  relationship previously reported (Lennernaes, 2007a). SVR for human was obtained to be 2.2 and this value was used in this study.

For the intestinal fluid volume ( $V_{\text{si}}$ ), 600 mL (8.6 mL/kg) has been reported for oral absorption simulation (Takano et al., 2006; Yu, 1999). On the other hand, Schiller et al. (2005) reported that the total volume of water pocket measured by water-sensitive magnetic resonance imaging is 105 mL in the human small intestine. However, this value might not be the real total volume available along the intestine, since only the free volume in the water pocket was counted (Lennernaes, 2007b). Biopharmaceutical classification system employs 250 mL (Yu et al., 2002). The same volume was also used to simulate the dose-dependent absorption of Gabapentin by active transport (Madan et al., 2005). Other reports also suggest smaller fluid volume than 600 mL (Macheras et al., 1990; Masaoka et al., 2006). In this study, the intestinal fluid volume was assumed to be 250 mL (36 mL in each compartment).

Numeric integration was performed by 4th Runge–Kutta method with integration interval of 0.5 min. The simulation programme was developed in-house utilizing Microsoft Excel Visual Basic Application (Microsoft Corporation, Redmont, WA).

## 4. Results and discussion

### 4.1. $F_a$ % prediction for danazol

The observed  $F_a$ % values of danazol in humans were obtained as follows (Table 1). Sunesen et al. (2005b) reported that the absolute bioavailability ( $BA\%_{\text{abs}}$ ) of a danazol capsule ( $d_{50} = 4.46 \mu\text{m}$ ) was 11% in fasted state, and the relative bioavailability against fed state ( $BA\%_{\text{rel}} = \text{AUC}(\text{fasted})/\text{AUC}(\text{fed})$ ) was 25%. Since  $BA\%_{\text{abs}} < F_a\% < BA\%_{\text{rel}}$ , it is appropriate to estimate  $F_a\% = 11$ –25% (The  $BA\%_{\text{rel}}$  was calculated from the AUCs of oral administration. Therefore, the first pass effect was cancelled out. However, oral absorption in the fed state could be incomplete and the AUC for complete absorption could be larger. Therefore,  $F_a\%$  is smaller than  $BA\%_{\text{rel}}$ ). In another report from Charman et al. (1993)  $BA\%_{\text{rel}}$  of a capsule dosed in the fasted state against the emulsion formation in the fed state was 23%. If i.v. data from Sunesen et al. was used,  $BA\%_{\text{abs}}$  was 19%. Therefore, it would be appropriate to estimate  $F_a\%_{\text{solid}} = 19$ –23%. Overall,  $F_a\%$  of a danazol capsule in fasted state humans would be 11–25%.  $F_a\%$  in the fed state was estimated in the same way to be 44–72%. The  $F_a\%$  of emulsion formation in the fed state was assumed to be 100%, because of the non-existence of dose independency in this formulation.

**Table 1**  
PK data of danazol in humans<sup>a</sup>.

Formulation	Dose (mg)	Fasted/fed	AUC (ng/(h <sup>-1</sup> mL <sup>-1</sup> ))	$BA\%_{\text{abs}}$	$BA\%_{\text{rel}}$
Solid <sup>a</sup>	100	Fasted	120 ± 60	11	14 <sup>b</sup> , 25 <sup>c</sup>
Solid <sup>a</sup>	100	Fed	469 ± 164	44	–
i.v. <sup>a</sup>	50		531 ± 104		
Solid <sup>d</sup>	100	Fasted	204 ± 125	19 <sup>e</sup>	23 <sup>b</sup>
Solid <sup>d</sup>	100	Fed	639 ± 259	60 <sup>e</sup>	72 <sup>b</sup>
Emulsion <sup>d</sup>	100	Fasted	779 ± 189	73 <sup>e</sup>	88 <sup>b</sup>
Emulsion <sup>d,f</sup>	100	Fed	844 ± 194	83 <sup>e</sup>	–
Emulsion <sup>d</sup>	50	Fed	296 ± 78	56 <sup>e</sup>	–
Emulsion <sup>d,f</sup>	100	Fed	695 ± 171	65 <sup>e</sup>	–
Emulsion <sup>d</sup>	200	Fed	1415 ± 303	67 <sup>e</sup>	–

<sup>a</sup> Data from Sunesen et al. (2005b).

<sup>b</sup> Relative  $BA\%$  against AUC of the emulsion formulation in the fed data.

<sup>c</sup> Relative  $BA\%$  against AUC of the fed data of the same study.

<sup>d</sup> Data from Charman et al. (1993).

<sup>e</sup> Calculated based on the i.v. data from Sunesen et al. (2005b).

<sup>f</sup> Different cohort.

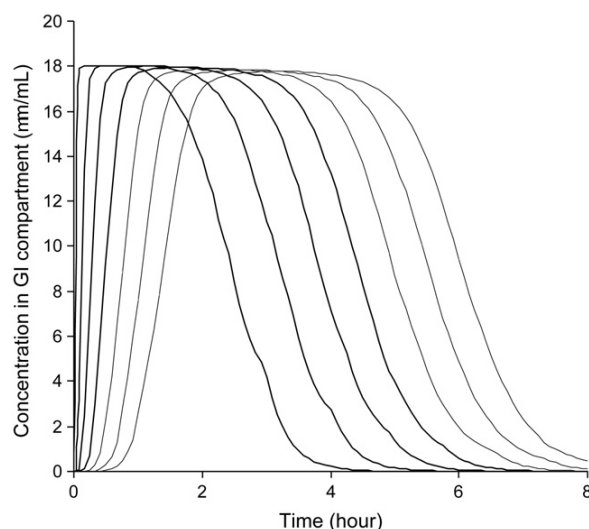


**Fig. 3.** Predicted concentration–time profile in the small intestine for danazol at 100 mg dose in fasted state humans. The numbers in the figure correspond to each small intestinal compartment (from left to right, compartment 1–7, proximal to distal, respectively).

The  $P_{\text{ep}}$  value of danazol, 0.098 cm/s, was obtained from the relationship between Caco-2 intrinsic permeability and  $\log P_{\text{oct}}$  (Fig. 2). In an in vitro system using plate wells, the apparent permeability is usually less than  $50 \times 10^{-6}$  cm/s since it is interfered with by the thick UWL. In an in vitro system, this UWL can be ca. 2000–4000  $\mu\text{m}$  depending on the agitation conditions (Avdeef et al., 2004; Fujikawa et al., 2007; Youdim et al., 2003). In the case of dissociable compounds, the intrinsic permeability can be obtained from the pH-permeability profile and  $pK_a$  data (Avdeef et al., 2005; Sugano, 2007). However, in the case of undissociable compounds such as danazol, this method can no be applied. Therefore,  $P_{\text{ep}}$  value for danazol was estimated by Eq. (7) using  $\log P_{\text{oct}}$ . Even though this was an estimated value, the estimation error had little effect on the prediction results, since the predicted  $P_{\text{ep,eff}}$  of danazol is much higher than UWL permeability which is less than  $10 \times 10^{-4}$  cm/s. The insensitivity of  $F_a\%$  (less than 3% difference) at the  $P_{\text{ep}}$  value of  $>0.01$  cm/s was confirmed (data not shown).

Log-normal distribution of particle size was assumed since only the  $d_{50}$  data was available. However, in the case of solubility limited absorption, such as in the case of danazol capsules, the estimation error of the dissolution rate has little effect on the  $F_a\%$  prediction (Sugano et al., 2007; Takano et al., 2006; Yu, 1999).

The SVR value obtained from the  $P_{\text{eff}}$ – $F_a\%$  relationship was 2.2. This value is higher than the theoretical value for a cylindrical tube ( $2/r_{\text{GI}} = 1.3$ ,  $r_{\text{GI}} = 1.5$  cm in humans) (Yu, 1999), suggesting that the intestinal tube is rather flat ( $DF = 1.7$ ) (Chiou, 1994).

In all simulation conditions, the calculated concentration in the small intestine reached the saturated solubility (Fig. 3). Although the mean  $T_{\text{si}}$  was set to be 3.5 h, the predicted concentration in the 6th and 7th compartments remained to be the saturated solubility until ca. 5 h, because a portion of the undissolved particles remain in the small intestine (Sugito et al., 1990) and maintain the saturated solubility.

Predicted  $P_{\text{eff}}$  and  $F_a\%$  in scenarios A–D are shown in Table 2. Scenario A largely underestimated  $F_a\%$  values. On the other hand, scenarios B and C resulted in good prediction. Scenario D largely overestimated  $F_a\%$ .

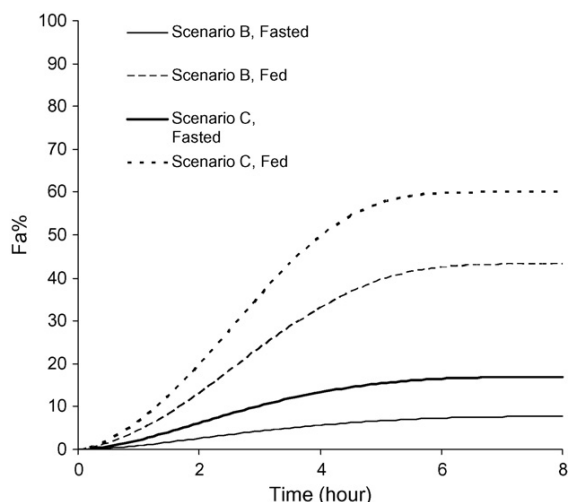
The  $F_a\%$ –time profiles predicted by scenarios B and C were also in good agreement with the previous results of Sunesen et al. (2005a) (Fig. 4).



**Table 2**

Simulation results for Fa% of danazol in humans (dose = 100 mg).

Fasted/fed	Scenario	Predicted $P_{eff}$ ( $\times 10^{-4}$ cm/s)	Predicted Fa%
Fasted	A (Eq. (3))	0.07	2
	B (Eq. (4))	0.44	8
	C (Eq. (5))	1.1	17
	D (Eq. (6))	8.0	62
Fed	A (Eq. (3))	0.04	2
	B (Eq. (4))	1.0	43
	C (Eq. (5))	1.6	60
	D (Eq. (6))	8.0	99

**Fig. 4.** Fa%–time profile predicted by scenarios B and C for danazol at 100 mg dose in fasted and fed state humans.

Recently, Persson et al. (2008) measured the  $P_{eff}$  of danazol dissolved in bile media using an intestinal perfusion model in pigs. Iso-osmotic solution was used to neglect water absorption. Therefore, the experimental condition corresponded to scenario B. The predicted  $P_{eff}$  value by scenario B ( $=0.44 \times 10^{-4}$  cm/s) in this study was in good agreement with the experimental result of ca.  $0.4 \times 10^{-4}$  cm/s in Persson's study.

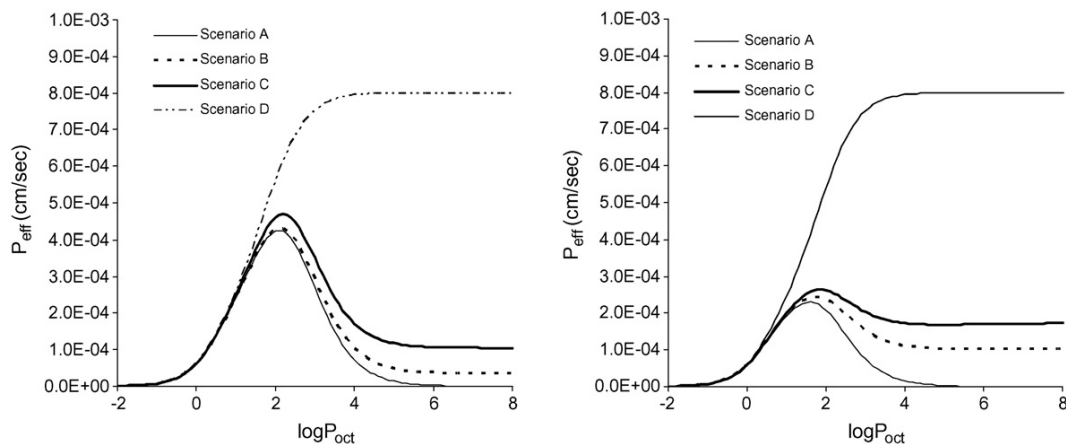
Even considering some uncertainty in input of physiological and compound parameters, scenarios B and C were suggested to be

more appropriate compared to scenarios A and D based on the large prediction error (Table 2). This was in good agreement with the previously proposed mechanism (Amidon et al., 1982; Araya et al., 2006; Li et al., 1996; Porter et al., 2007). However, more accurate estimation for the intestinal fluid volume, the UWL thickness, the diffusion coefficient of bile micelles in the mucus layer, the flatness of the intestinal tube, and the solubility in the intestinal fluid would be required to draw a conclusion about scenarios B and C from a simulation predictability aspect. In this study, danazol was used as a model drug, since all clinical pharmacokinetic data (solid dosage, p.o. solution and i.v.), particle size, solubility and physicochemical properties were available in the literature. The same conclusion was obtained for felodipine and danazol in dogs (manuscript under preparation).

Takano et al. previously employed scenario D for fasted state, and over estimation was also found for most low solubility compounds (e.g., for danazol, predicted Fa = 40%). However, the extent of over-estimation in their study is less than that in this study (Predicted Fa = 62%). In their simulation, they assumed a single compartment for the small intestine and at 4 h all particles exited the small intestine at once, whereas in this study it was suggested that a portion of particles remained in the small intestine for longer time than 4 h (Fig. 3).

#### 4.2. $\log P_{oct} - P_{eff}$ profile

Since both  $P_{ep}$  and  $K_{bm}$  can be predicted by  $\log P_{oct}$ ,  $\log P_{oct} - P_{eff}$  profile can be drawn (Fig. 5). This figure is not precisely quantitative due to the rough estimation of  $P_{ep}$  and  $K_{bm}$  by  $\log P_{oct}$ . For example,  $f_{mono}$  of danazol calculated by Eqs. (9) and (10) were 0.066 and 0.014 for FaSSiF and FeSSiF, respectively (experimental values were 0.012 and 0.0045). However, it would be beneficial to understand a general trend with a logarithmic scale. In  $\log P_{oct} < 2$  range, as  $\log P_{oct}$  increased,  $P_{eff}$  also increased. In this  $\log P_{oct}$  region, the epithelial membrane permeation would be the rate-limiting step. If bile micelle binding is not significant (corresponds to scenario D),  $P_{eff}$  increases up to ca.  $8 \times 10^{-4}$  cm/s at which the UWL limits permeability. However, if the bile micelle binding is significant as Eq. (10) predicts, as lipophilicity increased to over 2,  $P_{eff}$  decreases due to the increase of micelle binding (decrease of  $f_{mono}$ ). Micelle binding decreases both  $P_{UWL,eff}$  and  $P_{ep,eff}$  by reducing the effective diffusion coefficient and the free monomer fraction, respectively.  $P_{eff}$  value achieved a constant value of bile micelle permeation at  $\log P_{oct} > 4$ , because the power of the micelle partition equation (Eq.

**Fig. 5.**  $\log P_{oct}$  vs  $P_{eff}$  predicted by scenarios A–D for humans. (A) Fasted state, (B) fed state. TC = 3 mM and TC = 15 mM were used for the fasted state and fed state, respectively.  $P_{ep}$  and  $K_{bm}$  were calculated from  $\log P_{oct}$  by Eqs. (7) and (10), respectively.  $P_{eff}$  was calculated from  $P_{ep}$  and  $K_{bm}$  by Eqs. (2)–(6).  $D_{UWL,mono}$  was set to  $8 \times 10^{-6}$  cm<sup>2</sup>/s.

# Explore Litigation Insights

Docket Alarm provides insights to develop a more informed litigation strategy and the peace of mind of knowing you're on top of things.

## Real-Time Litigation Alerts



Keep your litigation team up-to-date with **real-time alerts** and advanced team management tools built for the enterprise, all while greatly reducing PACER spend.

Our comprehensive service means we can handle Federal, State, and Administrative courts across the country.

## Advanced Docket Research



With over 230 million records, Docket Alarm's cloud-native docket research platform finds what other services can't. Coverage includes Federal, State, plus PTAB, TTAB, ITC and NLRB decisions, all in one place.

Identify arguments that have been successful in the past with full text, pinpoint searching. Link to case law cited within any court document via Fastcase.

## Analytics At Your Fingertips



Learn what happened the last time a particular judge, opposing counsel or company faced cases similar to yours.

Advanced out-of-the-box PTAB and TTAB analytics are always at your fingertips.

## API

Docket Alarm offers a powerful API (application programming interface) to developers that want to integrate case filings into their apps.

## LAW FIRMS

Build custom dashboards for your attorneys and clients with live data direct from the court.

Automate many repetitive legal tasks like conflict checks, document management, and marketing.

## FINANCIAL INSTITUTIONS

Litigation and bankruptcy checks for companies and debtors.

## E-DISCOVERY AND LEGAL VENDORS

Sync your system to PACER to automate legal marketing.